

Heterologous Expression Facilitates the Production and Characterization of a Class III Lanthipeptide with Coupled Labionin Cross-Links in Sponge-Associated *Streptomyces rochei* MB037

Zhengjie Liu, Hao Li, Qianzhe Yu, Qianqian Song, Bo Peng, Kang Wang, and Zhiyong Li*



Cite This: *ACS Chem. Biol.* 2024, 19, 2060–2069



Read Online

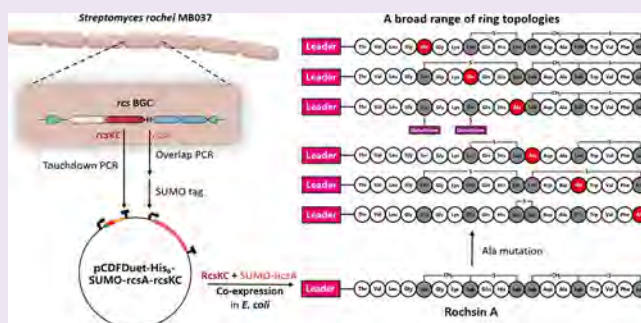
ACCESS |

Metrics & More

Article Recommendations

Supporting Information

ABSTRACT: Cyclic peptides, with remarkable stability, cellular permeability, and proteolysis resistance, display promising potential in pharmaceutical applications. Labionin (Lab), a unique bicyclic cross-link containing both C–C and C–S bonds, provides high rigidity and better control of conformation compared to monocyclic cross-links. To discover more Lab-containing scaffolds with highly rigid conformation for cyclic peptide drug development, herein, a cryptic class III lanthipeptide biosynthetic gene cluster (BGC) (i.e., *rcs*) was identified in the sponge-associated *Streptomyces rochei* MB037 and expressed in *Escherichia coli*, incorporating an N-terminal SUMO-tag on the RcsA precursor peptide to prevent proteolysis. Subsequently, a novel class III lanthipeptide, i.e., rochsin A, exhibiting a highly rigid conformation with coupled Lab cross-links crowded by bulky aromatic amino acids, was produced. Three AplP-like proteases outside the *rcs* BGC were proven to remove the leader peptide of rochsin A through their dual endo- and aminopeptidase activities, resulting in mature rochsin A *in vitro*. Ala mutation experiments revealed the C to N cyclization direction, like most class III lanthipeptides. However, RcsKC displays a high substrate breadth, enabling various ring topologies that are rarely observed in other class III lanthipeptides. Overall, the established expression system broadens the chemical diversity of cyclic peptides with unique Lab cross-links and offers a highly rigid scaffold for cyclic peptide drug development.



INTRODUCTION

Cyclic peptides, occupying a distinct niche between small-molecule drugs and large-molecule biologics due to their moderate size, display promising potential in pharmaceutical applications.¹ Compared with linear peptides, cyclic peptides are distinguished by their rigid structure, excellent stability, enhanced cellular permeability, robust resistance to protease, and more diverse three-dimensional shapes.² A number of approved cyclic peptide drugs are derived from natural products, e.g., cyclosporine, eptifibatid, and linaclotide, representing a treasure trove of novel therapeutic peptide leads.³ Lanthipeptides, a type of macrocyclic peptide, are part of the swiftly growing family of ribosomally synthesized and posttranslationally modified peptides (RiPP) natural products.⁴ Typically, linear peptides of ribosomal origin undergo post-translational modifications (PTMs) to achieve cyclization following the cleavage of the leader peptide, resulting in the production of final mature macrocyclic lanthipeptides. Unlike the classic disulfide bond (S–S) cyclization mode prominent in cyclic peptide drugs, lanthipeptides are cyclized by the metabolically stable thioether bond (C–S) of the lanthionine (Lan) cross-link (Figure S1).⁵ The substitution of disulfide bonds (S–S) with thioether bonds (C–S), formed by lanthipeptide synthetase, has been verified as a promising

strategy to enhance the bioactivity of disulfide-cyclized peptides, thereby exhibiting the significant therapeutic value of lanthipeptide.^{6,7}

Besides the Lan cross-link, some class III lanthipeptides feature a unique bicyclic labionin (Lab) cross-link, containing both C–S bonds and C–C bonds^{8,9} (Figure S1). Generally, bicyclic peptides present a more constrained conformation compared to monocyclic peptides, implying a higher binding affinity, specificity, and stability.¹⁰ The explosion of genomic data reveals abundant potential biosynthetic gene clusters (BGCs) for Lab-containing class III lanthipeptide,¹¹ but they are still underexplored, especially those derived from marine sources.¹² Moreover, the silencing characteristics of the BGCs in original strains under laboratory conditions, coupled with the high degradability of precursor peptides in heterologous expression hosts, greatly hinder the mining of Lab-containing compounds.¹³

Received: June 18, 2024

Revised: July 31, 2024

Accepted: August 12, 2024

Published: August 15, 2024



Microbes associated with marine organisms represent a promising trove for natural product discovery, and lanthipeptides derived from marine resources remain largely untapped.^{12,14} Sponges host diverse and abundant microbial symbionts, which are important sources of natural products and enzymes.^{15–19} The genome mining method avoids high rediscovery rates of known compounds, making the process more targeted and strategic, enabling focus on silent or underexpressed BGCs. With the aim of producing novel Lab-containing lanthipeptides with highly rigid structures from sponge symbiotic microbes, this study activated a cryptic class III lanthipeptide BGC (*rsc*) in the sponge-associated *Streptomyces rochei* MB037 by heterologous expression of *rsc* BGC in *E. coli*, embedding a SUMO-tag at the N-terminus of the precursor peptide to avoid proteolysis. Consequently, a novel lanthipeptide, termed rochsins A, was successfully obtained, presenting a highly rigid structure with coupled Lab cross-links crowded by bulky aromatic amino acids. Since the *rsc* BGC lacks a protease gene for leader peptide removal, we explored unclustered proteases to handle this process and obtain the mature rochsins A. Meanwhile, *in vivo* Ala mutation experiments were applied to analyze the cyclization direction and substrate promiscuity.

RESULTS

Discovery of Class III Lanthipeptide Biosynthetic Gene Cluster. *S. rochei* MB037 was isolated from the marine sponge *Dysidea arenaria* in the South China Sea.²⁰ A series of borrelidin analogues were identified through precursor feeding²¹ and coculture strategies.²² In order to further explore the potential of secondary metabolite synthesis by *S. rochei* MB037, we analyzed the genome using antismash 6.0.²³ A cryptic class III lanthipeptide biosynthetic gene cluster (BGC) was found and named *rsc*, which was supposed to produce compound rochsins. The *rsc* BGC (12 kb) in *S. rochei* MB037 contains two precursor peptide genes *rscA1/2*, a supposed class III lanthipeptide synthetase gene *rscKC*, a FtsX-like permease, two ABC transporters and two regulatory genes (Figure 1A).

To better understand the composition of *rsc* BGCs and precursor sequence conservation, we analyzed similar BGCs using the RcsA1/2 as a query in BLASTP and identified 12 additional *rsc*-like BGCs in 12 bacterial genomes from nonredundant protein sequences (NR) database (Figure 1B and Figure S2). Among the 13 BGCs, we observed that 3 of them contained the genes annotated as protease, hydrolase, and peptidase from *Streptomyces* sp. Rer75 (CP058693.1), *Streptomyces* sp. MMBL 11–1 (CP117709.1), and *Kitasatospora xanthocidica* JCM 4862 (NZ_BNBY01000001.1), respectively. The N-terminal leader peptide (LP) of RcsA contains an LLDLQE motif, which is highly conserved in the class III lanthipeptide leader sequence. The C-terminal core peptide (CP) contains two SxxSxx(x)C motifs that have the potential to form labionin (Lab) or lanthionine (Lan) cross-link. In particular, the CP has a highly rigid structure. On one hand, these two SxxSxx(x)C motifs (x represents a random amino acid) are directly adjacent, with no gap of even one amino acid in between, implying coupled Lab or Lan cross-links. On the other hand, the SxxSxx(x)C motifs are crowded with bulky aromatic amino acids, presenting large steric hindrance that might further fix the rigid conformation. Moreover, the WVF motif in the second SxxSxx(x)C motifs is also reminiscent of those in labyrinthopeptin A1 (WVPF),

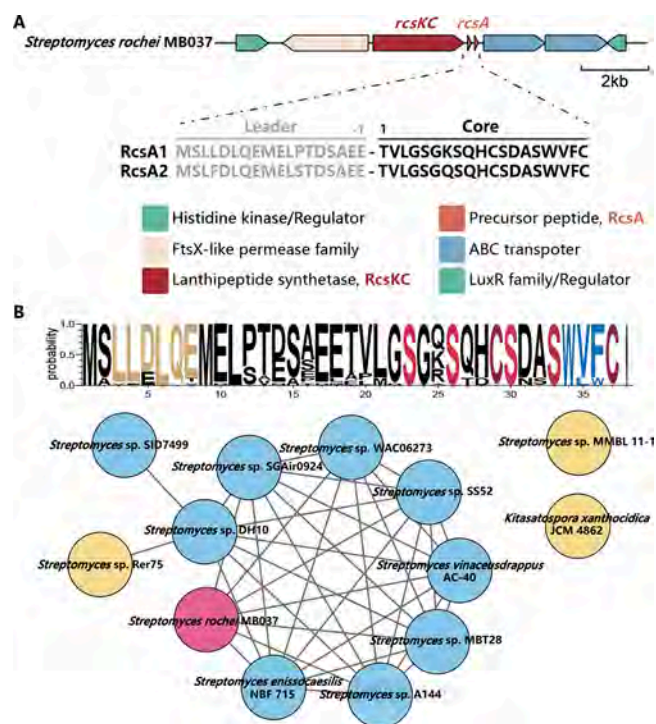


Figure 1. Organization of *rsc* BGC in this study and the similarity network of *rsc*-like BGCs in the NR database. (A) The *rsc* BGC from *S. rochei* MB037, displaying genes and the RcsA1/2 amino acid sequences. In standard RiPP nomenclature, the first amino acid of the core peptide is labeled as residue (1), and the final amino acid of the leader peptide is designated as residue (–1). (B) Sequence logo of the RcsA in *rsc*-like BGCs and the *rsc*-like BGCs similarity network constructed by BiG-SCAPE²⁴ (cutoffs = 0.3). The *S. rochei* (this study) are colored in purple and bacteria containing protease in their *rsc* BGCs are colored in beige.

the first representative class III lanthipeptide exhibits significant antiviral activity.⁸

Reconstitution of the *rsc* BGC Produces Rochsins A. Our previous studies^{20–22} did not detect any putative precursor peptides in the culture extracts of *S. rochei* MB037 (Figure S3), which suggests that the *rsc* BGC is silent or low-yielding under standard laboratory conditions. Hence, we applied the heterologous coexpression strategy to reconstitute this *rsc* BGC by introducing only the RcsKC synthetase and RcsA precursor peptide into *E. coli*, aiming to activate the production of rochsins (Figure 2A).

Considering the limited difference between the two precursors RcsA1 and RcsA2 (with only one amino acid difference in the core peptide region), we selected to clone solely the codon-optimized *rscA1* using overlap PCR to streamline the process for further identification. The expression plasmid pCDFDuet-His₆-RcsA-RcsKC was transformed into *E. coli* BL21 (DE3), which was then cultured in LB medium and induced with IPTG. After induction, the cells were harvested by centrifugation following further purification and characterization steps. Unfortunately, we failed to obtain full-length modified His₆-RcsA1 by NiNTA purification. However, the extraction with MeOH followed by high-resolution LC-MS, yielded truncated and modified RcsA1 (–4 H₂O) with a mass of [M+3H]³⁺ = 1014.7765 (exp: [M+3H]³⁺ = 1014.7737, ppm = 2.75) (Figure S4). This phenomenon suggests the peptide sequence might be cleaved

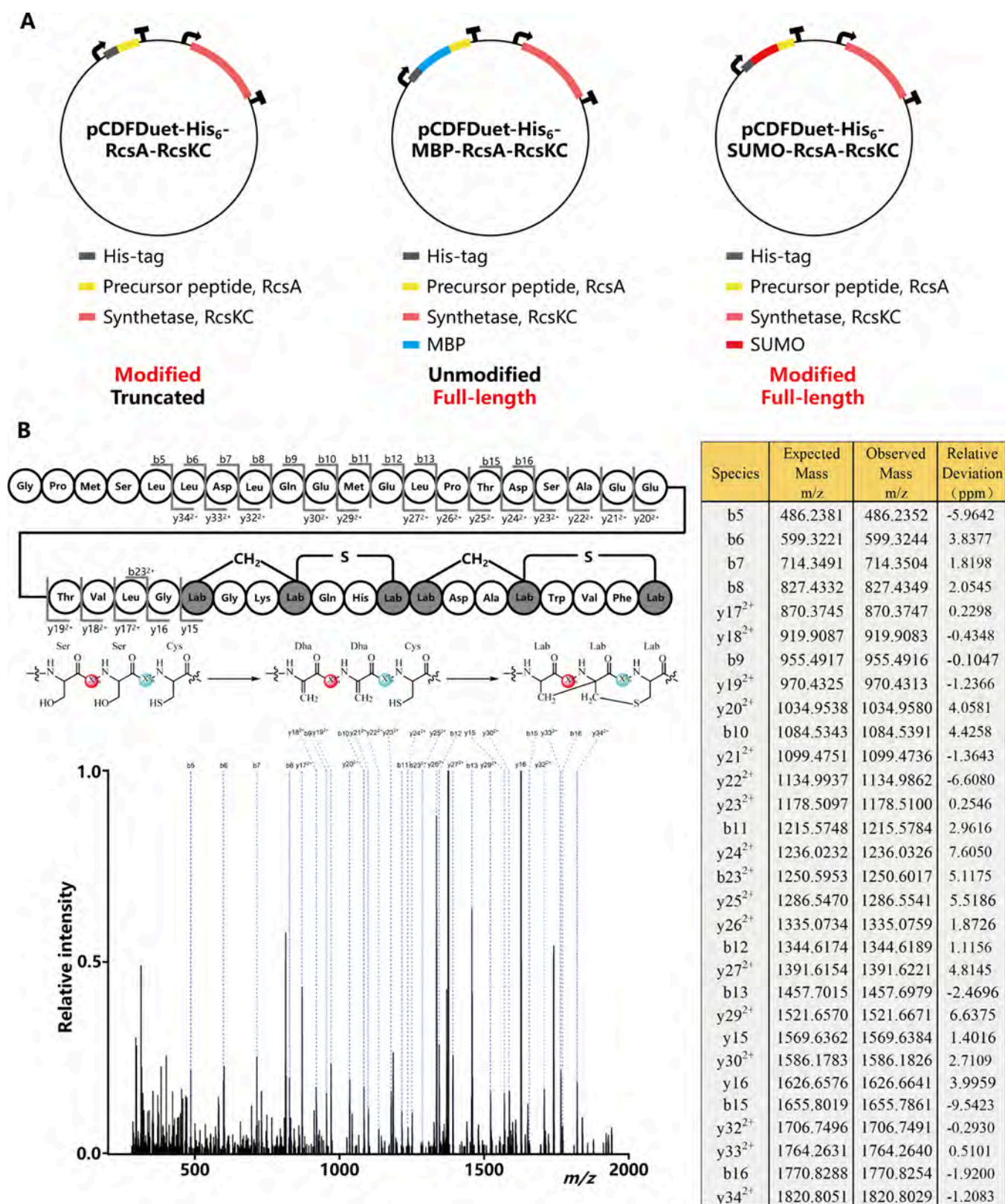


Figure 2. Overview of the RcsA1 and RcsKC coexpression systems. (A) Results of three different RcsA1 (His₆-RcsA1, His₆-MBP-RcsA1, His₆-SUMO-RcsA1) coexpressed with RcsKC. The modified and full-length RcsA1 (rochsin A) was obtained only when the SUMO-tag was used. (B) The proposed structure of rochsin A, along with CID-MS/MS fragmentation pattern and MS/MS spectra using the SUMO-tag removed by PreScission Protease. Absent fragments in the region of Ser5-Cys19 indicate the location of the Lab rings. MBP: maltose binding protein; SUMO: small ubiquitin-like modifier.

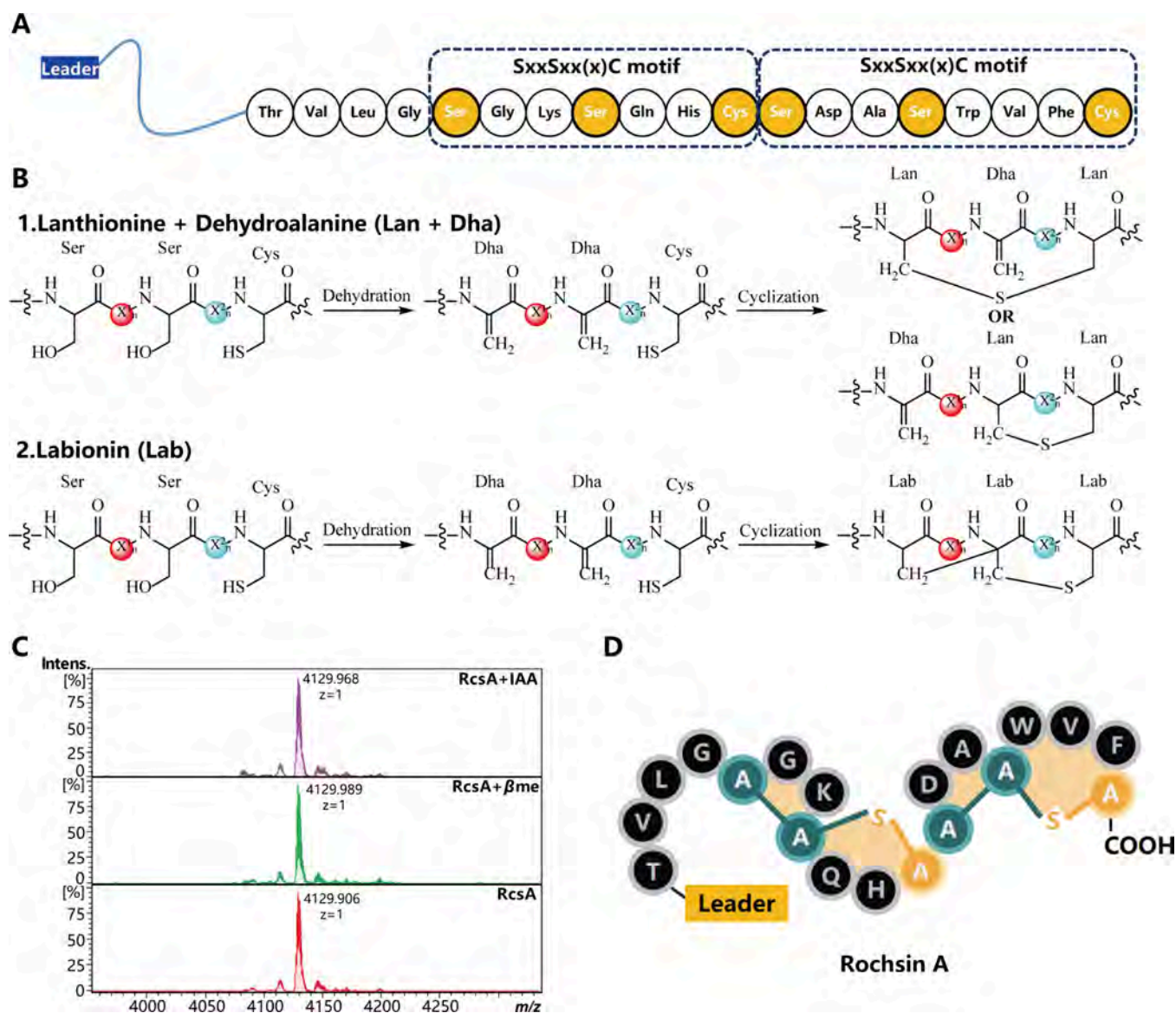


Figure 3. Structure characterization of rochsin A. (A) Amino acid sequence of RcsA1. The two conserved SxxSxx(x)C motifs are marked in the figure. (B) The structures of Lan + Dha moiety and Lab moiety that are characterized in class III lanthipeptides. (C) MALDI-TOF MS analysis of rochsin A treated with IAA and β ME. No β ME and IAA adduct was observed. (D) The proposed structure of rochsin A with Lab cross-links colored in a faint yellow shade. Segments originating from Ser are in green, segments originating from Cys are in orange.

by the endogenous protease of *E. coli*.^{25,26} In an effort to enhance the stability of RcsA in *E. coli* and obtain the full-length modified precursor, we constructed the His₆-MBP-RcsA1 and RcsKC coexpression system. Using the N-terminal MBP-tagged RcsA1 to prevent nonspecific proteolysis, we observed the presence of unmodified full-length RcsA1 rather than the modified form, as determined by MALDI-TOF MS analysis (Figure S5). Given the possibility that the bulky size of MBP might impede the interaction between RcsKC and RcsA1, we altered MBP to SUMO, a smaller tag, to shield the precursor peptide from hydrolysis. Following this idea, we reconstructed the coexpression system via His₆-SUMO-RcsA1 and RcsKC. In this way, modified full-length RcsA1 (−4 H₂O) (i.e., rochsin A) was obtained with a yield of ~1 mg/L LB (obs: [M+3H]³⁺ = 1375.9557, exp: [M+3H]³⁺ = 1375.9501, ppm = 4.07).

Structural Characterization and Bioactivity Evaluation of Rochsin A. A triply charged ion of [M+3H]³⁺ =

1375.9557 (exp: [M+3H]³⁺ = 1375.9501, ppm = 4.07) corresponding to the rochsin A was observed using LC-HRMS (Figure S6). MS/MS analysis confirmed the composition of leader peptide in rochsin A, and the absence of detectable fragments in the Ser₅-Cys₁₉ region suggests the presence of Lab or Lan + Dha moiety, formed by the two conserved SxxSxx(x)C motifs in the core peptide (Figure 2B and Figure 3A). To investigate the presence of Lab and Lan + Dha moiety (Figure 3B), we employed a chemical derivatization assay with β -mercaptoethanol (β ME) and iodoacetamide (IAA) to quantify the number of free Dha and Cys residues in the structure,²⁷ respectively. However, no β ME and IAA adducts were observed, suggesting that all Dha and Cys residues were involved in the ring formation (Figure 3C). In other words, the core peptide of rochsin A contains only the Lab moiety (Figure 3D). Subsequently, we performed hydrolysis and *N*-trifluoroacetyl/ethyl ester derivatization following LC-HRMS analysis,^{28–30} to further confirm the

existence of the Lab moiety. Results showed an ion at m/z 668.1328 (exp: 668.1324, ppm = 0.60) corresponding to the Lab derivative and no Lan derivative was detected, confirming that rochsin A consists of Lab cross-links (Figures S7 and S8).

Before the NMR analyses, we applied GluC protease for rochsin truncation to simplify the spectra (Figure S9). Under the scrutiny of 1D NMR spectra, two diagnostic signals were identified, with two quaternary sp^3 -hybridized carbons ($\delta_C = 59.8$ and 61.2 for the resonances of Lab8/15) confirming the existence of Lab moieties in this entity (Figures S10–S13). Due to highly overlapped NMR signals and the limited amount of sample, elucidation of the 2D NMR cross-peaks were hindered (Figures S14–S17). Antimicrobial and cytotoxicity tests of truncated rochsin A were also performed. No significant antimicrobial or cytotoxic activity was observed, but it can act as a morphogen, like SapB,³¹ facilitating the morphological differentiation of *S. rochei* MB037 (Figure S9 and Table S1)

Unclustered Protease Completes Leader Peptide Removal. Similar to the majority of class III lanthipeptide BGCs,³² the *rsc* BGC in the *S. rochei* MB037 genome lacks a protease gene responsible for leader peptide removal. Proteases located outside the *rsc* BGC were employed for the cleavage of the leader peptide, the final step in compound maturation. To identify the actual protease involved in leader cleavage, we initially investigated the homologues of the genes, annotated as protease, hydrolase, and peptidase in the *rsc*-like BGCs in the genome of *S. rochei* MB037 (Figure S18). Taking these genes as a query, four homologues (StrR037P1–StrR037P4) were detected using the Basic Local Alignment Search Tool (BLAST) and three of them were soluble when expressed in the *E. coli* BL21(DE3) with pET28a. However, we only observed StrR037P2 exhibited cleavage activity to unmodified RcsA2 obtained by solid phase peptide synthesis (Figure 4) and no truncated modified RcsA1 (rochsin A) was detected, even when the reaction time was extended to 48 h.

Subsequently, we investigated the cleavage activity of AplP-like protease, which was previously reported as an effective strategy for removing leader peptide of class III/IV lanthipeptides.^{26,33} Three AplP homologues, named StrR037P5–7, were discovered in the genome of *S. rochei*

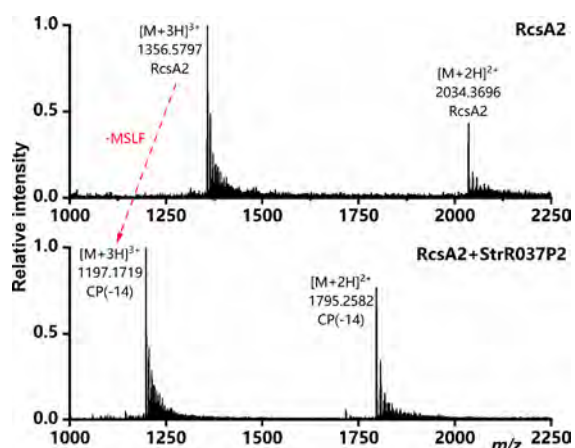


Figure 4. Cleavage activity of StrR037P2 to unmodified RcsA2. CP (Core peptide) is followed by numbers indicating the position of the cleavage site. RcsA2: $[M+3H]^{3+} = 1356.5797$ (exp: $[M+3H]^{3+} = 1356.5812$, ppm = -1.11); CP(-14): $[M+3H]^{3+} = 1197.1719$ (exp: $[M+3H]^{3+} = 1197.1728$, ppm = -0.75).

MB037, and then expressed in *E. coli* BL21(DE3) with pET28a. Three soluble proteins were obtained following activity verification *in vitro*. Within the initial 24 h of the reaction, we observed full-length modified RcsA1 (rochsin A) as well as relatively long-digested fragments, indicating the endopeptidase activity of StrR037P5–7 (Figure 5, Figure S19,

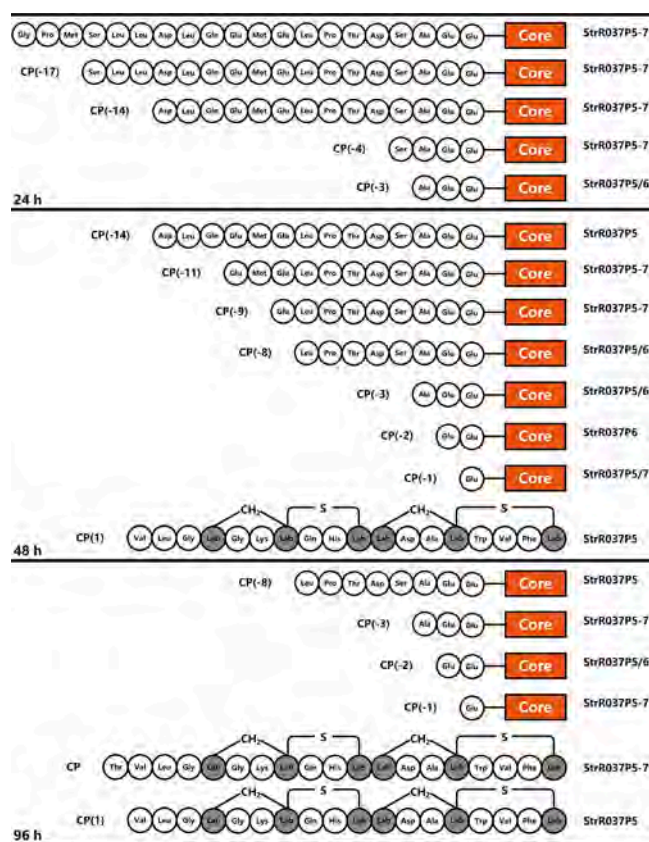


Figure 5. Cleavage activity of StrR037P5–7 for modified RcsA1. CP (Core peptide) is followed by numbers indicating the position of cleavage site.

and Table S2). As the reaction time was prolonged, the initially formed peptides were further degraded to shorter fragments through the aminopeptidase activity of StrR037P5–7. Similar phenomena have been observed in other class III lanthipeptides, such as erythreapeptin,³⁴ avermipeptin,³⁴ and labyrinthopeptin,⁸ where the final peptide products were identified with different leader peptide overhangs. In addition, the unmodified precursor peptide was also efficiently cleaved by AplP-like protease, suggesting that the C-terminal ring is unrelated to the proteolytic efficiency of the AplP-like protease. Overall, the unclustered bifunctional AplP-like proteases exhibit both endo- and aminopeptidase activities on both modified and unmodified precursor peptides.

Cyclization Direction and Substrate Promiscuity of the Reconstituted *rsc* BGC. The abovementioned *in vivo* coexpression system of His₆-SUMO-RcsA1 and RcsKC facilitated a more in-depth assessment of cyclization direction and substrate promiscuity. Herein, six mutants were generated in which a single amino acid was substituted by alanine. Each mutant was subjected to detailed MS/MS analysis following β ME and IAA derivatized treatment to investigate the ring pattern of each mutant (Figure 6; Figures S20–S26). Comparing the substitutions of Ala in the N-terminal Lab

Peptides	Sequence	+ IAA (free Cys)	+ β ME (free Dha)
WT		0	0
S5A		0	0
S8A		0	0
S8A + 1GSH		1	0
C11A + 2GSH		0	0
S12A 2H2O		0	0
S15A		0	1
S15A 2H2O		0	0
C19A		0	3
C19A 3H2O		0	2
Truncated S12A			

Figure 6. Results of RcsA variant peptides (Ser/Cys \rightarrow Ala) using the *in vivo* coexpression system of His₆-SUMO-RcsA and RcsKC. The mutants, not fully dehydrated or reacted with GSH, are marked with the corresponding number of H₂O or GSH below. Altered ring patterns are highlighted in orange and green light.

(S5A, S8A, and C11A) with those in the C-terminal Lab (S12A, S15A, and C19A), the mutation in the N-terminal Lab (S5A, S8A, and C11A) did not affect the formation of C-terminal Lab (Figure 6). However, the disturbance of the C-terminal Lab ring (S12A, S15A, and C19A) altered the N-terminal ring pattern. This suggests that the formation of C-terminal Lab serves as a prerequisite for N-terminal Lab formation, implying a C to N directionality for cyclization like a mostly class III lanthipeptides.^{30,35,36} In addition, the truncated precursor peptides, like the proteolytic LP(-2) fragment in S12A (Figure 6), were present in all C-terminal mutants but rare in N-terminal mutants.

The dehydration of RcsA was also partly affected by the disturbance of the C-terminal Lab, as undehydrated Ser5 was detected in S12A, S15A, and C19A variants. Moreover, because *E. coli* is comparatively high in glutathione (GSH), sometimes even more than 10 mM,³⁷ GSH adducts are commonly found in the heterologous expression system of *E. coli*.^{38,39} For RcsA, GSH adducts were also detected in the S8A

and C11A mutants. Finally, a mini Lan ring was detected in the C19A mutant, where the Cys11 residue reacted with the Dha12 residue in the opposite direction, a phenomenon rarely observed in class III lanthipeptides.

Overall, the above results reveal the C to N cyclization direction, as observed in most class III lanthipeptides. However, RcsKC displays high substrate promiscuity *in vivo*, enabling the production of various ring topologies that are rarely observed in other class III lanthipeptides.

DISCUSSION

Class III lanthipeptides, a rapidly expanding subclass of lanthipeptides, represent an underexplored treasure trove of new natural products, offering distinct chemical scaffolds and broad biological activities. The bicyclic labionin cross-link, exclusive to class III lanthipeptides, distinguishes them from all other classes of lanthipeptides and makes them important in expanding the chemical diversity of cyclic peptides. As previously indicated,^{13,26} proteolysis by endogenous proteases

remains a major obstacle to the production of class III or IV lanthipeptide BGCs in *E. coli*. Adding protein tags is an effective strategy to improve the stability of precursor peptides.⁴⁰ Here, we compared three different expression systems and found that SUMO tags alone can reduce peptide degradation by *E. coli* endogenous proteases without affecting cyclization, thereby highlighting the feasibility and priority of SUMO tags in class III lanthipeptide BGCs production. Consequently, a novel lanthipeptide, i.e., rochsin A, characterized by a highly rigid structure featuring coupled Lab cross-links with bulky aromatic amino acids, was produced. Unlike other reported Lab-containing lanthipeptides, the Lab cross-links in rochsin A are directly adjacent, with no amino acid functioning as a flexible linker between the two rigid Lab cross-links⁴¹ (Figure 3D).

Given the absence of the protease gene in BGCs and the limited functionality of commercial proteases, it is of great significance to develop a universal protease for leader peptide removal in class III lanthipeptides. RiPPs always remain inactive unless the leader peptide is removed.⁴² To identify the actual protease for leader removal, we initially identified an unclustered StrR037P2 through genome mining but only observed its cleavage activity on the unmodified RcsA2 (Table S3). Meanwhile, three AplP homologues were found to be capable of conducting leader peptide removal by their dual endo- and aminopeptidase activities, thereby verifying the feasibility of the AplP in marine bacterial and showing its potential as a universal method for leader peptide removal in class III lanthipeptides.³³

Finally, Ala mutation experiments revealed the C to N cyclization direction, like most class III lanthipeptides. However, RcsKC displayed a high substrate breadth, enabling the production of various ring topologies that are rarely observed in other class III lanthipeptides. Compared with the representative stackpeptin, known for its higher substrate promiscuity than other reported class III lanthipeptides,³⁶ C-terminal mutations in StaA completely abolish its cyclization. In contrast, all RcsA mutants were capable of ring formation, irrespective of whether the mutations were introduced at the C-terminus or N-terminus, indicating the potentially high substrate promiscuity of RcsKC (Figure 6). Further observation found the truncated precursor peptides, like proteolytic LP(-2) fragment in S12A, were present in all C-terminal mutants, but rare in N-terminal mutants, implying the potential impact of C-terminal mutation. Cyclization and proteolysis appear to be competing processes that together determine the fate of RcsA *in vivo*. The cyclized RcsA is resistant to degradation of the endogenous proteases in *E. coli*. However, if the cyclization process slows down, the precursor peptide may be degraded by proteases before cyclization is completed, resulting in a truncated peptide. Hence, the stabilization provided by the SUMO-tag and the rigid conformation of the core peptide might play a key role in this high substrate promiscuity of RcsKC *in vivo*.

Totally, this study broadens the chemical diversity of cyclic peptides with the unique coupled Lab cross-links. The established coexpression system fosters deeper exploration of promising natural products from underexplored marine resources and provides new insights into cyclic peptide engineering.

MATERIALS AND METHODS

Bacterial Strains and Genome Mining. *S. rochei* MB037 (China Center for Type Culture Collection (CCTCC), accession number AA 2017041) was isolated from the sponge *Dysidea arenaria* around Yongxin Island in the South China Sea.²⁰ Antismash 6.0²³ with default parameters was utilized to identify potential BGCs in the genome assembly of *S. rochei* MB037 and to predict the boundary between the leader and core peptide of RcsA (the precursor peptides of rcs BGC). The sequence similarity network of rcs-like BGCs was analyzed using BiG-SCAPE²⁴ with RcsA1/2 as the query in a BLASTP search against the NR database. The sequence logo for RcsA in rcs-like BGCs was generated using WebLogo.⁴³

Construction of pCDFDuet-RcsA-RcsKC Coexpression Plasmids. The codon-optimiztic gene of His₆-RcsA1 peptides was obtained by overlap PCR using RcsA_P1-4 primers listed in Table S4 and inserted into the first cloning site (*NcoI/HindIII* site) of pCDFDuet-1 plasmids to generate pCDFDuet-His₆-RcsA1 plasmids. The rcsKC gene was cloned from the genomic DNA of *S. rochei* MB037 using the RcsKC_F/R primers listed in Table S4 by touchdown PCR and inserted into the second cloning site (*NdeI/AvrII* site) of pCDFDuet-His₆-RcsA1 plasmids. The amino acid sequence of RcsKC is given in Table S5. The MBP and SUMO tags were individually inserted in front of the rcsA1 gene of pCDFDuet-His₆-RcsA1-RcsKC using Gibson assembly, resulting in the generation of pCDFDuet-His₆-MBP-RcsA1-RcsKC and pCDFDuet-His₆-SUMO-RcsA1-RcsK, respectively.

Heterologous Expression in *Escherichia coli* BL21 (DE3). The expression plasmid was transformed into the *E. coli* BL21 (DE3), which was then cultured at 37 °C in LB medium containing 50 mg/L streptomycin to an OD₆₀₀ of 0.6–0.8 and induced with IPTG at a final concentration of 0.3 mM at 18 °C for an additional 22 h. The cells were harvested by centrifugation at 4500 rpm for 20 min.

Preparation and Purification of Rochsin A. To obtain rochsin A (including leader peptide and modified core peptide), previously reported purification approaches were adopted with slight modifications.⁴⁰ After centrifugation at 4500 rpm for 20 min, the collected cell pellets were resuspended in 15 mL of lysis buffer (10 mM imidazole, 300 mM NaCl, 50 mM HEPES, 10% glycerol, pH 7.5) and lysed using sonication in an ice water bath. Cell debris was removed by centrifugation at 12000 rpm for 40 min at 18 °C, and the resulting supernatant was filtered through a 0.45 μm filter prior to being loaded onto a pre-equilibrated 5 mL HisTrap HP (GE Healthcare). The column was washed with 25 mL of wash buffer (25 mM imidazole, 300 mM NaCl, 50 mM HEPES, 10% glycerol, pH 7.5) and then eluted with 20 mL of elution buffer (120 mM imidazole, 300 mM NaCl, 50 mM HEPES, 10% glycerol, pH 7.5). Desired proteins were determined visually by sodium dodecyl sulfate polyacrylamide gel electrophoresis (SDS-PAGE), and the buffer was exchanged three times with PreScission Protease cleavage buffer (50 mM Tris-HCl, 150 mM NaCl, 1 mM EDTA, 1 mM DTT, pH 7.5) before concentration using an Amicon Ultra Centrifugal Filter Unit (10 kDa MWCO, Millipore).

To remove the SUMO/MBP tag, proteolysis was performed at 4 °C for 16 h by the addition of 1:100 (*w:w*) PreScission Protease before adding equal volumes of acetonitrile (ACN) precipitated the SUMO/MBP tag. Precipitated proteins were eliminated by centrifugation at 14000 rpm for 10 min and the resultant supernatant was subjected to MALDI-TOF MS or LC-MS analysis. Further purification was performed by preparative HPLC with an RP-C18 column (Eclipse XDB-C18, 9.4 × 250 mm, 5 μm), monitored at a UV absorbance of 220 nm and flow rate of 4 mL/min. A gradient elution was employed with solvent A (10 mM NH₄HCO₃ in Milli-Q water) and solvent B (10 mM NH₄HCO₃ in 80% ACN) as follows: *T* = 0 min, 90% solvent A; *T* = 5 min, 90% solvent A; *T* = 28 min, 10% solvent A; *T* = 31 min, 10% solvent A; *T* = 33 min, 90% solvent A; *T* = 35 min, 90% solvent A. The desired fraction containing rochsin A was identified using MALDI-TOF MS following lyophilization for complete dryness.

β ME Derivatization for Dha Residue Quantification. The peptides were treated with 10 mM β ME in 50 mM NH_4HCO_3 at 37 °C for 1 h. Also, the reactions were further desalted using ZipTipC18 following MALDI-TOF MS analysis.

IAA Derivatization for Free Cys Residue Quantification. The peptides were incubated with 20 mM IAA and 0.1 mM TCEP in 50 mM NH_4HCO_3 at RT in the dark for 30 min. Subsequently, the resulting mixture was desalted using a ZipTipC18 following MALDI-TOF MS analysis.

Preparation and Purification of the Truncated Rochsin A. The purified rochsin A was dissolved in Milli-Q water containing 50 mM NH_4HCO_3 . GluC protease was then added, and the mixture was allowed to react at 37 °C for 16 h. Subsequently, an equal volume of ACN was added followed by repeated freeze–thaw centrifugation. The supernatant was collected for the second preparative HPLC. In the second preparative HPLC, the solvent composition was altered, with solvent A consisting of Milli-Q water with 0.1% trifluoroacetic acid and solvent B composed of ACN with 0.1% trifluoroacetic acid, while the remaining parameters remained unaltered. Similarly, the desired fraction containing core peptide was identified using MALDI-TOF MS following lyophilization for complete dryness.

NMR Data Acquisition. The truncated rochsin A was dissolved in 500 μL of $\text{DMSO-}d_6$. The ^1H , ^{13}C , DEPT-135, COSY, NOESY, HSQC, and HMBC spectra were collected on a Bruker AVANCE III HD 700 MHz spectrometer.

Determination of Labionin by Hydrolysis and Derivatization. The determination of labionin was carried out using a modified strategy according to ref 28. Rochsin A (1 mg) was dissolved in a 6 M hydrochloric acid solution (2 mL) and subjected to hydrolysis at 110 °C for 24 h under high pressure. After cooling to RT, the hydrochloric acid was removed by purging with N_2 gas. Upon drying, the hydrolysate was redissolved in 500 μL of 2 M ethanolic HCl-solution, prepared from acetyl chloride in ethanol (1:4, *v:v*), and was heated for 30 min at 110 °C following drying again with N_2 gas. The resulting products were incubated in dichloromethane (200 μL) and trifluoroacetic anhydride (100 μL) at 110 °C for 20 min before another drying step under N_2 gas. The final residue was dissolved in 100 μL of MeOH and subjected to LC-MS analysis.

Unclassified Protease to Remove the Leader Peptide of Rochsin A. The putative protease genes were obtained by touchdown PCR from the genome of *S. rochei* before being inserted into the pET28a plasmid. The primers and amino acid sequences are listed in Tables S4 and S5, respectively. Transformation and expression induction procedures are similar to those in Part 2.3, with only antibiotics replaced by ampicillin. Recombinant *E. coli* BL21(DE3) cells were harvested by centrifugation and resuspended with buffer S (500 mM NaCl, 20 mM Tri-HCl, 10% glycerol, pH 8.0) following disruption by sonication. Cell debris was removed by centrifugation. Then, the supernatant was loaded onto the 5 mL of HisTrap HP pre-equilibrated with buffer A (30 mM imidazole, 500 mM NaCl, 20 mM Tri-HCl, pH 8.0). The column was washed with five volumes of buffer A before a linear gradient from buffer A to 100% buffer B (500 mM imidazole, 500 mM NaCl, and 20 mM Tri-HCl, pH 8.0). Desired fractions were determined by SDS-PAGE and the buffer was exchanged thrice with buffer C (500 mM NaCl, 20 mM Tri-HCl, 10% glycerol, 350 μM β ME, pH 8.0) using an Amicon Ultra Centrifugal Filter Unit (10 kDa MWCO, Millipore). Finally, the enzyme solution was stored at –80 °C for further use.

To remove the leader peptide, the *in vitro* reaction system (100 μL) consisted of 100 μM purified rochsin A and 10 μM protease in 20 mM Tris-HCl buffer at pH 7.5, maintained at RT. In the control, the protease was replaced with an equal volume of ddH_2O . LC-MS analysis was performed after quenching the reaction with an equal volume of methanol.

Site-Directed Mutagenesis. All of the RcsA mutants were generated by PCR using the pCDFDuet-His₆-SUMO-RcsA1-RcsK plasmid as the template. The mutagenic primers are listed in Table S4. The PCR reaction system for site-directed mutagenesis included 20 ng of plasmids template, 0.2 μM of each primer, 25 μL of 2 \times Phanta Flash Master Mix (DNA polymerase), 1 μL of DMSO, and sterile

ddH_2O to bring the final volume to 50 μL . The PCR procedure was as follows: (98 °C for 10 s, 55 °C for 5 s, 72 °C for 35 s) \times 28 cycles. The resulting mixture was digested with DpnI for 3 h before being transformed into *E. coli* BL21(DE3) for sequencing verification and subsequent expression.

■ ASSOCIATED CONTENT

Supporting Information

The Supporting Information is available free of charge at <https://pubs.acs.org/doi/10.1021/acscchembio.4c00428>.

Information of primers, Rcs-like BGCs and mass spectrometric data; the draft genome sequence of *S. rochei* MB037 is deposited in the NCBI database under PRJNA1108166 (PDF)

■ AUTHOR INFORMATION

Corresponding Author

Zhiyong Li – Marine Biotechnology Laboratory, State Key Laboratory of Microbial Metabolism and School of Life Sciences and Biotechnology, Shanghai Jiao Tong University, Shanghai 200240, China; Yazhou Bay Institute of Deepsea Science and Technology, Shanghai Jiao Tong University, Shanghai 200240, P.R. China; Email: zyli@sjtu.edu.cn

Authors

Zhengjie Liu – Marine Biotechnology Laboratory, State Key Laboratory of Microbial Metabolism and School of Life Sciences and Biotechnology, Shanghai Jiao Tong University, Shanghai 200240, China; orcid.org/0009-0007-7688-6636

Hao Li – Marine Biotechnology Laboratory, State Key Laboratory of Microbial Metabolism and School of Life Sciences and Biotechnology, Shanghai Jiao Tong University, Shanghai 200240, China

Qianzhe Yu – Marine Biotechnology Laboratory, State Key Laboratory of Microbial Metabolism and School of Life Sciences and Biotechnology, Shanghai Jiao Tong University, Shanghai 200240, China

Qianqian Song – Marine Biotechnology Laboratory, State Key Laboratory of Microbial Metabolism and School of Life Sciences and Biotechnology, Shanghai Jiao Tong University, Shanghai 200240, China

Bo Peng – Marine Biotechnology Laboratory, State Key Laboratory of Microbial Metabolism and School of Life Sciences and Biotechnology, Shanghai Jiao Tong University, Shanghai 200240, China

Kang Wang – Marine Biotechnology Laboratory, State Key Laboratory of Microbial Metabolism and School of Life Sciences and Biotechnology, Shanghai Jiao Tong University, Shanghai 200240, China

Complete contact information is available at:

<https://pubs.acs.org/doi/10.1021/acscchembio.4c00428>

Author Contributions

All authors have given approval to the final version of the manuscript.

Notes

The authors declare no competing financial interest.

■ ACKNOWLEDGMENTS

This work was funded by the National Key Research and Development Program of China (2022YFC2804101) and the

Sanya Science and Technology Innovation Special Project (2022KJCX63). We appreciate Prof. Qianjin Kang and Prof. Wei Ding from SJTU for their valuable suggestions. We also thank the Core Facility and Service Center for the School of Life Sciences and Biotechnology at SJTU for their instrumental support.

REFERENCES

- (1) Morrison, C. Constrained peptides' time to shine? *Nat. Rev. Drug Discovery* **2018**, *17*, 531–533.
- (2) Zhang, H.; Chen, S. Cyclic peptide drugs approved in the last two decades (2001–2021). *RSC Chem. Biol.* **2022**, *3*, 18–31.
- (3) Muttenthaler, M.; King, G. F.; Adams, D. J.; Alewood, P. F. Trends in peptide drug discovery. *Nat. Rev. Drug Discovery* **2021**, *20*, 309–325.
- (4) Ongpipattanakul, C.; Desormeaux, E. K.; DiCaprio, A.; van der Donk, W. A.; Mitchell, D. A.; Nair, S. K. Mechanism of action of ribosomally synthesized and post-translationally modified peptides. *Chem. Rev.* **2022**, *122*, 14722–14814.
- (5) Repka, L. M.; Chekan, J. R.; Nair, S. K.; van der Donk, W. A. Mechanistic understanding of lanthipeptide biosynthetic enzymes. *Chem. Rev.* **2017**, *117*, 5457–5520.
- (6) Zhao, X.; Kuipers, O. P. Nisin- and ripcin-derived hybrid lanthipeptides display selective antimicrobial activity against *Staphylococcus aureus*. *ACS Synth. Biol.* **2021**, *10*, 1703–1714.
- (7) Zhao, X.; Xu, Y.; Viel, J. H.; Kuipers, O. P. Semisynthetic macrocyclic lipo-lanthipeptides display antimicrobial activity against bacterial pathogens. *ACS Synth. Biol.* **2021**, *10*, 1980–1991.
- (8) Meindl, K.; Schmiederer, T.; Schneider, K.; Reicke, A.; Butz, D.; Keller, S.; Gühring, H.; Vértessy, L.; Wink, J.; Hoffmann, H.; Brönstrup, M.; Sheldrick, G. M.; Süßmuth, R. D. Labyrinthopeptins: a new class of carbacyclic lantibiotics. *Angew. Chem. Int. Ed.* **2010**, *49*, 1151–4.
- (9) Li, Y.; Ma, Y.; Xia, Y.; Zhang, T.; Sun, S.; Gao, J.; Yao, H.; Wang, H. Discovery and biosynthesis of tricyclic copper-binding ribosomal peptides containing histidine-to-butyryne crosslinks. *Nat. Commun.* **2023**, *14*, 2944.
- (10) Kong, X. D.; Moriya, J.; Carle, V.; Pojer, F.; Abriata, L. A.; Deyle, K.; Heinis, C. De novo development of proteolytically resistant therapeutic peptides for oral administration. *Nat. Biomed Eng.* **2020**, *4*, 560–571.
- (11) Xue, D.; Older, E. A.; Zhong, Z.; Shang, Z.; Chen, N.; Dittenhauser, N.; Hou, L.; Cai, P.; Walla, M. D.; Dong, S. H.; Tang, X.; Chen, H.; Nagarkatti, P.; Nagarkatti, M.; Li, Y. X.; Li, J. Correlational networking guides the discovery of unclustered lanthipeptide protease-encoding genes. *Nat. Commun.* **2022**, *13*, 1647.
- (12) Paoli, L.; Ruscheweyh, H. J.; Forneris, C. C.; Hubrich, F.; Kautsar, S.; Bhushan, A.; Lotti, A.; Claysen, Q.; Salazar, G.; Milanese, A.; Carlström, C. I.; Papadopoulou, C.; Gehrig, D.; Karasikov, M.; Mustafa, H.; Larralde, M.; Carroll, L. M.; Sánchez, P.; Zayed, A. A.; Cronin, D. R.; Acinas, S. G.; Bork, P.; Bowler, C.; Delmont, T. O.; Gasol, J. M.; Gossert, A. D.; Kahles, A.; Sullivan, M. B.; Wincker, P.; Zeller, G.; Robinson, S. L.; Piel, J.; Sunagawa, S. Biosynthetic potential of the global ocean microbiome. *Nature*. **2022**, *607*, 111–118.
- (13) Ayikpoe, R. S.; Shi, C.; Battiste, A. J.; Eslami, S. M.; Ramesh, S.; Simon, M. A.; Bothwell, I. R.; Lee, H.; Rice, A. J.; Ren, H.; Tian, Q.; Harris, L. A.; Sarkisian, R.; Zhu, L.; Frerk, A. M.; Precord, T. W.; van der Donk, W. A.; Mitchell, D. A.; Zhao, H. A scalable platform to discover antimicrobials of ribosomal origin. *Nat. Commun.* **2022**, *13*, 6135.
- (14) Carroll, A. R.; Copp, B. R.; Davis, R. A.; Keyzers, R. A.; Prinsep, M. R. Marine natural products. *Nat. Prod. Rep.* **2021**, *38*, 362–413.
- (15) Li, Z., *Symbiotic microbiomes of coral reefs sponges and corals*. Springer Nature: New York, 2019.
- (16) Li, Y.; Zhang, F.; Banakar, S.; Li, Z. Bortezomib-induced new bergamotene derivatives xylariterpenoids H-K from sponge-derived fungus *Pestalotiopsis maculans* 16F-12. *RSC Adv.* **2019**, *9*, 599–608.
- (17) Li, Y.; Li, Z. Cyclopeptide Derivatives from the Sponge-Derived Fungus *Acremonium persicinum* F10. *Mar. Drugs* **2021**, *19*, 537.
- (18) Liu, C.; Xiao, Y.; Xiao, Y.; Li, Z. Marine urease with higher thermostability, pH and salinity tolerance from marine sponge-derived *Penicillium steckii* S4–4. *Marine life science & technology*. **2021**, *3*, 77–84.
- (19) Valliappan, K.; Sun, W.; Li, Z. Marine actinobacteria associated with marine organisms and their potentials in producing pharmaceutical natural products. *Appl. Microbiol. Biotechnol.* **2014**, *98*, 7365–77.
- (20) Karuppiah, V.; Li, Y.; Sun, W.; Feng, G.; Li, Z. Functional gene-based discovery of phenazines from the actinobacteria associated with marine sponges in the South China Sea. *Appl. Microbiol. Biotechnol.* **2015**, *99*, 5939–50.
- (21) Li, Y.; Zhang, F.; Banakar, S.; Li, Z. Comprehensive optimization of precursor-directed production of BC194 by *Streptomyces rochei* MB037 derived from the marine sponge *Dysidea arenaria*. *Appl. Microbiol. Biotechnol.* **2018**, *102*, 7865–7875.
- (22) Yu, M.; Li, Y.; Banakar, S. P.; Liu, L.; Shao, C.; Li, Z.; Wang, C. New metabolites from the co-culture of marine-derived actinomycete *Streptomyces rochei* MB037 and fungus *Rhinochrysiella similis* 35. *Front. Microbiol.* **2019**, *10*, 915.
- (23) Blin, K.; Shaw, S.; Kloosterman, A. M.; Charlop-Powers, Z.; van Wezel, G. P.; Medema, M. H.; Weber, T. AntiSMASH 6.0: improving cluster detection and comparison capabilities. *Nucleic Acids Res.* **2021**, *49*, W29–w35.
- (24) Navarro-Muñoz, J. C.; Selem-Mojica, N.; Mallowney, M. W.; Kautsar, S. A.; Tryon, J. H.; Parkinson, E. I.; De Los Santos, E. L. C.; Yeong, M.; Cruz-Morales, P.; Abubucker, S.; Roeters, A.; Lokhorst, W.; Fernandez-Guerra, A.; Cappellini, L. T. D.; Goering, A. W.; Thomson, R. J.; Metcalf, W. W.; Kelleher, N. L.; Barona-Gomez, F.; Medema, M. H. A computational framework to explore large-scale biosynthetic diversity. *Nat. Chem. Biol.* **2020**, *16*, 60–68.
- (25) Guo, S.; Wang, S.; Ma, S.; Deng, Z.; Ding, W.; Zhang, Q. Radical SAM-dependent ether crosslink in daropeptide biosynthesis. *Nat. Commun.* **2022**, *13*, 2361.
- (26) Ren, H.; Shi, C.; Bothwell, I. R.; van der Donk, W. A.; Zhao, H. Discovery and characterization of a class IV lanthipeptide with a nonoverlapping ring pattern. *ACS Chem. Biol.* **2020**, *15*, 1642–1649.
- (27) Ayikpoe, R. S.; van der Donk, W. A. Peptide backbone modifications in lanthipeptides. *Methods Enzymol.* **2021**, *656*, 573–621.
- (28) Pesic, A.; Henkel, M.; Süßmuth, R. D. Identification of the amino acid labionin and its desulfurised derivative in the type-III lantibiotic LabA2 by means of GC/MS. *ChemComm.* **2011**, *47*, 7401–3.
- (29) Xue, D.; Shang, Z.; Older, E. A.; Zhong, Z.; Pulliam, C.; Peter, K.; Nagarkatti, M.; Nagarkatti, P.; Li, Y. X.; Li, J. Refactoring and heterologous expression of class III lanthipeptide biosynthetic gene clusters lead to the discovery of *N,N*-dimethylated lantibiotics from Firmicutes. *ACS Chem. Biol.* **2023**, *18*, 508–517.
- (30) Wang, H.; van der Donk, W. A. Biosynthesis of the class III lanthipeptide catenulipeptin. *ACS Chem. Biol.* **2012**, *7*, 1529–35.
- (31) Kodani, S.; Hudson, M. E.; Durrant, M. C.; Buttner, M. J.; Nodwell, J. R.; Willey, J. M. The SapB morphogen is a lantibiotic-like peptide derived from the product of the developmental gene ramS in *Streptomyces coelicolor*. *Proc. Natl. Acad. Sci. U.S.A.* **2004**, *101*, 11448–53.
- (32) Zhang, Q.; Doroghazi, J. R.; Zhao, X.; Walker, M. C.; van der Donk, W. A. Expanded natural product diversity revealed by analysis of lanthipeptide-like gene clusters in actinobacteria. *Appl. Environ. Microbiol.* **2015**, *81*, 4339–50.
- (33) Chen, S.; Xu, B.; Chen, E.; Wang, J.; Lu, J.; Donadio, S.; Ge, H.; Wang, H. Zn-dependent bifunctional proteases are responsible for leader peptide processing of class III lanthipeptides. *Proc. Natl. Acad. Sci. U.S.A.* **2019**, *116*, 2533–2538.
- (34) Völler, G. H.; Krawczyk, J. M.; Pesic, A.; Krawczyk, B.; Nachtigall, J.; Süßmuth, R. D. Characterization of new class III lantibiotics—erythreapeptin, avermipeptin and griseopeptin from

Saccharopolyspora erythraea, *Streptomyces avermitilis* and *Streptomyces griseus* demonstrates stepwise N-terminal leader processing. *Chem-BioChem*. **2012**, *13*, 1174–83.

(35) Jungmann, N. A.; Krawczyk, B.; Tietzmann, M.; Ensle, P.; Süßmuth, R. D. Dissecting reactions of nonlinear precursor peptide processing of the class III lanthipeptide curvopeptin. *J. Am. Chem. Soc.* **2014**, *136*, 15222–8.

(36) Jungmann, N. A.; van Herwerden, E. F.; Hügelland, M.; Süßmuth, R. D. The supersized class III Lanthipeptide stackepeptin displays motif multiplication in the core peptide. *ACS Chem. Biol.* **2016**, *11*, 69–76.

(37) Lee, H.; Wu, C.; Desormeaux, E. K.; Sarkisian, R.; van der Donk, W. A. Improved production of class I lanthipeptides in *Escherichia coli*. *Chem. Sci.* **2023**, *14*, 2537–2546.

(38) Vermeulen, R.; Van Staden, A. D. P.; van Zyl, L. J.; Dicks, L. M. T.; Trindade, M. Unusual class I lanthipeptides from the marine bacteria *Thalassomonas viridans*. *ACS Synth Biol.* **2022**, *11*, 3608–3616.

(39) Han, Y.; Wang, X.; Zhang, Y.; Huo, L. Discovery and characterization of marinsedin, a new class II lanthipeptide derived from marine bacterium *Marinicella sediminis* F2(T). *ACS Chem. Biol.* **2022**, *17*, 785–790.

(40) Hegemann, J. D.; van der Donk, W. A. Investigation of substrate recognition and biosynthesis in class IV lanthipeptide systems. *J. Am. Chem. Soc.* **2018**, *140*, 5743–5754.

(41) Hegemann, J. D.; Süßmuth, R. D. Matters of class: coming of age of class III and IV lanthipeptides. *RSC Chem. Biol.* **2020**, *1*, 110–127.

(42) Oman, T. J.; van der Donk, W. A. Follow the leader: the use of leader peptides to guide natural product biosynthesis. *Nat. Chem. Biol.* **2010**, *6*, 9–18.

(43) Crooks, G. E.; Hon, G.; Chandonia, J. M.; Brenner, S. E. WebLogo: a sequence logo generator. *Genome Res.* **2004**, *14*, 1188–90.